

ChemComm

Chemical Communications

Accepted Manuscript

This article can be cited before page numbers have been issued, to do this please use: S. M. Ghoreishian, M. Norouzi and J. Lauterbach, *Chem. Commun.*, 2025, DOI: 10.1039/D4CC06382A.



This is an Accepted Manuscript, which has been through the Royal Society of Chemistry peer review process and has been accepted for publication.

Accepted Manuscripts are published online shortly after acceptance, before technical editing, formatting and proof reading. Using this free service, authors can make their results available to the community, in citable form, before we publish the edited article. We will replace this Accepted Manuscript with the edited and formatted Advance Article as soon as it is available.

You can find more information about Accepted Manuscripts in the [Information for Authors](#).

Please note that technical editing may introduce minor changes to the text and/or graphics, which may alter content. The journal's standard [Terms & Conditions](#) and the [Ethical guidelines](#) still apply. In no event shall the Royal Society of Chemistry be held responsible for any errors or omissions in this Accepted Manuscript or any consequences arising from the use of any information it contains.

1 **Recent progress in the decomposition of ammonia as potential hydrogen-**
2 **carrier by green technologies**

3

4 **Seyed Majid Ghoreishian, Mohammad Norouzi, Jochen Lauterbach***5 ^a *Department of Chemical Engineering, University of South Carolina, Columbia, SC 29208,*
6 *USA.*7 ^b *School of Cancer Sciences, University of Glasgow, Glasgow, UK.*

8

9 *Corresponding author

10 E-mail address: lauteraj@cec.sc.edu (J. Lauterbach)

1 Abstract

2 To meet the global carbon neutrality target set by the United Nations, finding alternative and
3 cost-effective energy sources has become prominent while enhancing energy conversion
4 methods' efficiency. The versatile applications of hydrogen (H₂) as an energy vector have been
5 highly valued over the past decades due to its significantly lower greenhouse gas emissions
6 compared to conventional fossil fuels. However, challenges related to H₂ generation and
7 storage for portable applications have increasingly called attention to ammonia (NH₃)
8 decomposition as an effective method of on-site hydrogen production due to its characteristic
9 high hydrogen content, high energy density, and affordability. This review highlights recent
10 developments in green decomposition techniques of ammonia, including catalytic membrane
11 reactors, microchannel reactors, thermochemical processes, non-thermal plasma, solar-driven
12 decomposition, and electrolysis, with a focus on the latest developments in new methods and
13 materials (catalysts, electrodes, and sorbents) employed in these processes. Moreover,
14 technical challenges and recommendations are discussed to assess the future potential of
15 ammonia in the energy sector. The role of machine learning and artificial intelligence in
16 ammonia decomposition is also emphasized, as these tools open up ways of simulating
17 reaction mechanisms for the exploration of a new generation of high-performance catalysts
18 and reduce trial-and-error approaches.

19
20 **Keywords:** Hydrogen, Renewable energy, Catalysis, Ammonia decomposition, Activity.



Table of Contents

1		
2		
	1. Introduction	4
	2. Photocatalysis	10
	3. Electrocatalysis	18
	4. Plasma	26
	5. Other	31
	6. Predicting NH ₃ decomposition efficiency by machine learning	32
	7. Further challenges for ammonia decomposition	34
	8. Conclusions and Perspectives	35
	Data availability	36
	Conflicts of interest	36
	Acknowledgements	36
	References	37

3



1 1. Introduction

2 The demand for global energy has increased due to a highly energy-intensive lifestyle and the
3 continuing growth of the world's population ¹. Currently, approximately 733 million people
4 globally lack access to electricity, while 2.4 billion people lack clean fuels and modern cooking
5 technologies ². According to the Energy Institute Statistical Review of World Energy 2023,
6 fossil fuels, coal, oil, and natural gas are still the main primary energy sources (82%) ³. There
7 is a broad consensus that fossil fuel reserves, particularly oil, are on the verge of depletion and
8 shortage by the end of this century ⁴. Due to the continuous reliance on fossil fuels, a substantial
9 amount of greenhouse gases (GHGs) such as CO₂, CO, SO₂, NO_x, and volatile organic
10 compounds (mainly CO₂) has been emitted into Earth's atmosphere ⁵⁻⁸. CO₂ is recognized as
11 the primary driver of global warming, with approximately 80% originating from the
12 combustion of fossil fuels within the industrial sector ⁹. To respond to global climate change
13 and meet the Paris Agreement's temperature control goals, there is a worldwide consensus on
14 reducing greenhouse gas emissions toward net-zero carbon emissions ⁹. In this context, China
15 has set a target to reach "peak carbon" by 2030 and "carbon neutrality" by 2060 ¹⁰.

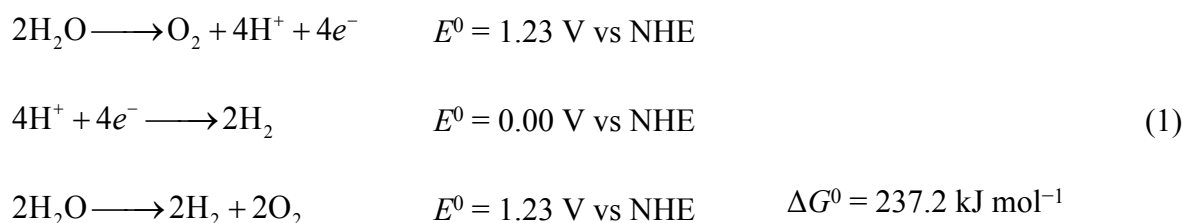
16 Renewable energy technologies, including solar and wind power, are increasingly achieving
17 cost parity with conventional fossil fuel-based energy sources ¹¹. However, as these energy
18 sources are intermittent and unevenly distributed across the globe, they are still complex to
19 replace traditional energy completely ¹². Therefore, hydrogen (H₂) has been drawn to our
20 attention as a new energy source without pollution or CO₂ emissions.

21 Hydrogen, with the smallest relative molecular mass, is of significant interest as a secondary
22 energy source due to its high gravimetric energy density (~33 kWh kg⁻¹), which is greater than
23 that of either gasoline or diesel fuel, and its capacity for zero-emission output ^{13, 14}. The U.S.
24 Department of Energy (DOE) initially set hydrogen storage targets in 2009 for applications
25 such as portable power, onboard light-duty vehicles, and material-handling equipment. The

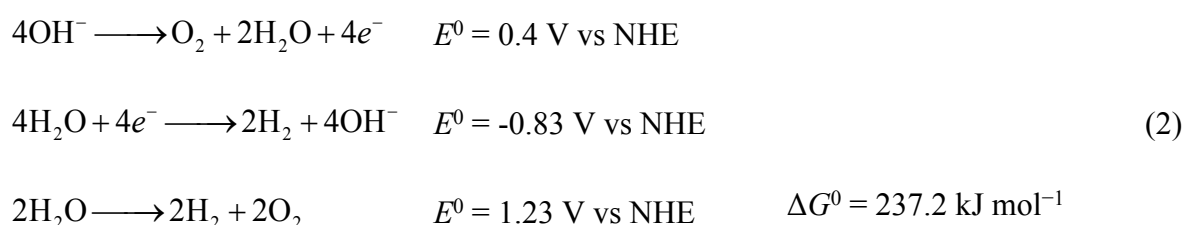


1 DOE set specific targets for on-board hydrogen storage: 0.030 kg H₂ L⁻¹ and 4.5 wt % for
 2 volumetric and gravimetric storage capacities by 2020¹⁵. In addition, China is actively working
 3 to increase its production of carbon-neutral hydrogen (green hydrogen) to meet its carbon
 4 neutrality goals, which involves water splitting (Eqs. 1-2) to extract hydrogen using electricity
 5 generated from renewable sources such as wind and solar energies^{9, 16}. It is expected that till
 6 2025, the specific system targets aim for 1.8 kWh kg⁻¹ system (0.055 kg H₂ kg⁻¹ system), 1.3
 7 kWh L⁻¹ system (0.040 kg H₂ L⁻¹), and \$9 kWh⁻¹ storage system (\$300 kg⁻¹ stored H₂ system).

8 In acidic solution



In alkaline solution



9
 10 Currently, hydrogen can be stored in carbon fiber tanks at high pressures (>35 MPa), achieving
 11 a gravimetric H₂ capacity of 0.025 kg H₂ kg⁻¹ system at 350 bar¹⁷. Hydrogen can only be
 12 liquefied at extremely low temperatures of -253 °C or pressures above 70 MPa that
 13 significantly increase the costs associated with the storage and transportation of hydrogen
 14 energy⁹. Therefore, the transportation and storage of hydrogen remains a critical barrier,
 15 significantly impeding its industrial applications¹⁴.



1 One potential solution to address hydrogen transport issues involves the utilization of liquid or
2 solid hydrogen energy carriers, from which hydrogen is chemically extracted upon arrival. The
3 selection of a hydrogen energy carrier focuses on environmental friendliness, efficiency, ease
4 of handling and transport, and a high hydrogen mass and volume percentage. Given that,
5 methanol and ammonia are frequently discussed as the feasible carriers.⁹

6 Accordingly, ammonia (NH₃) possesses high H₂ content (17.8 wt%) and a large energy density
7 (3000 Wh kg⁻¹). It has greater volumetric hydrogen density than liquid H₂ (121 kg H₂ m⁻³) and
8 can be liquefied and stored at room temperature, facilitating the transportation and storage,
9 particularly in the liquid phase, as NH₃ gas is liquefied under a pressure of 8.5 MPa at 20 °C
10^{18, 19}. Notably, hydrogen produced through ammonia decomposition typically contains fewer
11 impurities compared to hydrogen derived from hydrocarbons (like methanol)²⁰.

12 Ammonia decomposition has been mainly investigated since the 19th century¹⁸. In 1904,
13 Perman and Atkinson reported that complete decomposition of ammonia is not achievable
14 below 1100 °C. They also noted that the degree of decomposition depends significantly on the
15 nature of the surface in contact with the ammonia, particularly the catalysts involved²⁰. To
16 date, various metals, alloys, and their compounds (such as oxides and nitrides) have been
17 extensively studied as active catalysts for NH₃ decomposition. Given that ammonia
18 decomposition is the exact reverse of industrial ammonia synthesis from nitrogen and
19 hydrogen, the microkinetic principle suggests that catalysts effective for NH₃ generation
20 should, in theory, facilitate ammonia decomposition. However, the catalytic activity trends
21 differ significantly between the two processes due to their opposing reaction pathways and
22 targeted products²¹.

23 Prior to 1990, Fe-based catalysts attracted significant interest, however, in the past decade,
24 research has increasingly shifted toward noble metal catalysts, with growing attention on metal
25 nitrides, carbides, and alloys as active components for the decomposition reaction²². Till now,



1 various monometallic systems based on non-noble metals have been investigated for hydrogen
2 production from ammonia. Over the last decade, the catalytic decomposition of NH_3 over
3 catalysts such as platinum (Pt), palladium (Pd), ruthenium (Ru), and rhodium (Rh) has gained
4 a lot of attention in substitution of iron¹⁸. While, these metals show outstanding activities, their
5 large-scale applications significantly increase the cost, which is a substantial drawback²³. To
6 tackle this issue, transition metal carbides (MoC_x , VC_x , WC_x , and FeC_x) and nitrides (MoN_x ,
7 VN_x , and WN_x), along with zirconium oxynitride have been recruited. Amidst those,
8 molybdenum nitride and tungsten carbide have received the most attention in ammonia
9 decomposition studies. Notably, these catalysts are generally evaluated under conditions
10 relevant not only to hydrogen production but also to gasification mixture clean-up²⁴. For
11 bimetallic catalysts, several studies have been explored, including Ni–Pt, Ni/Ru, Pd/Pt/Ru/La,
12 and Fe– MO_x ($M = \text{Ce}, \text{Al}, \text{Si}, \text{Sr}, \text{and Zr}$). However, a key challenge for bimetallic catalysts
13 remains the structural stability of these catalysts under reaction conditions, particularly
14 concerning metal segregation. This could lead to increased energy consumption, creating
15 potential obstacles for the decomposition of NH_3 ²⁵. Given that enhanced metal interactions
16 appear to contribute to higher catalytic activity, optimizing preparation methods and selecting
17 appropriate metal salts could offer promising strategies for improving performance²⁶.
18 Research has shown that alloying strategy can play a crucial role in facilitating ammonia
19 decomposition reaction to their monometallic counterparts by improving the catalytic
20 performance of catalysts^{25, 27}. In this area, a broad range of alloy systems has developed,
21 including Co alloys with Ni²⁸, Re²⁹ and Ce³⁰, Ni alloys with Co, Fe, and Cu³¹, Ru–Ni³², Cu–
22 Zn³³, etc. These findings demonstrate that alloy-based catalysts could provide a more cost-
23 effective alternative while preserving—or even exceeding—the catalytic efficiency of noble
24 metals³⁴. However, choosing the right elements and appropriate stoichiometric composition
25 remains a significant challenge for NH_3 decomposition over alloyed catalysts to ensure both



1 optimal activity and long-term stability³⁵. Therefore, one of the most significant challenges in
 2 the preparation of hydrogen from ammonia decomposition is to customize an effective catalyst
 3 that is energy efficient, highly selective, scalable, and affordable, providing a stable rate of
 4 decomposition at low temperatures³⁶.

5 Recent researches have shifted focus from Ru-based catalysts to alternative transition metal
 6 (TM) and TM-free catalysts. Among these, alkali amides and imides, particularly lithium-based
 7 compounds such as LiNH₂ and Li₂NH, have demonstrated a significant reduction in activation
 8 barriers by stabilizing M–N bond intermediates. Theoretical studies further highlight the
 9 importance of surface disorder dynamics in non-stoichiometric lithium amide compounds (Li₂-
 10 _x(NH₂)_x(NH)_{1-x}) for TM-free catalysis, suggesting mechanistic differences from TM-based
 11 systems. Similar to TM-free NH₃ synthesis catalysts, lithium amides/imides exhibit catalytic
 12 activity for ammonia decomposition both with and without transition metals. Notably, addition
 13 of TM to LiNH₂ enhances NH₃ conversion at 440 °C from 54% to 86%, in which catalytic
 14 performance was also influenced by ammonia flow rates³⁷. Table 1 provides a summary of the
 15 most effective heterogeneous catalysts used for the thermal decomposition of ammonia.

16
 17 **Table 1.** The most effective heterogeneous catalysts utilized for the decomposition of ammonia
 18 ¹⁸.

Catalyst	Temperature (°C)	Conversion (%)	TOF (1/s)	Ref.
Ni/MgAl ₂ O ₄ – LDH	600	88.7	2.18	38
Co/NC-600	500	80		39
Ru/SmCeO _x	400	74.9	25.81	40
35Co/BHA	500	87.2		41
2.5Ru/10 C-rGO	400	96	75.4	42



CoRe _{1.6}	500	~90		29 View Article Online DOI: 10.1039/D4CC06382A
K ⁺ -Fe/C	470	20	~0.5	43
Ru/Al ₂ O ₃	580		6.85	44
20Co–10Ni/Y ₂ O ₃	550	71.2		45
Co-containing CNTs	700	~100		46
Ni-10/ATP	650	64.3		47
α-FeO ₂ O ₃ -50 @pSiO ₂	800	100		48
10%Co/MWCNTs	600		8.15	49
Ru/La _{0.33} Ce _{0.67}	450	91.9	11.4	50
Ni ₅ Co ₅ /SiO ₂	550	76.8		28
5CMLa-5	550	82.7		51
1%K-Co/SiC	350	33.1	9.3	52
Pr-Ni/Al ₂ O ₃	550	~90		53

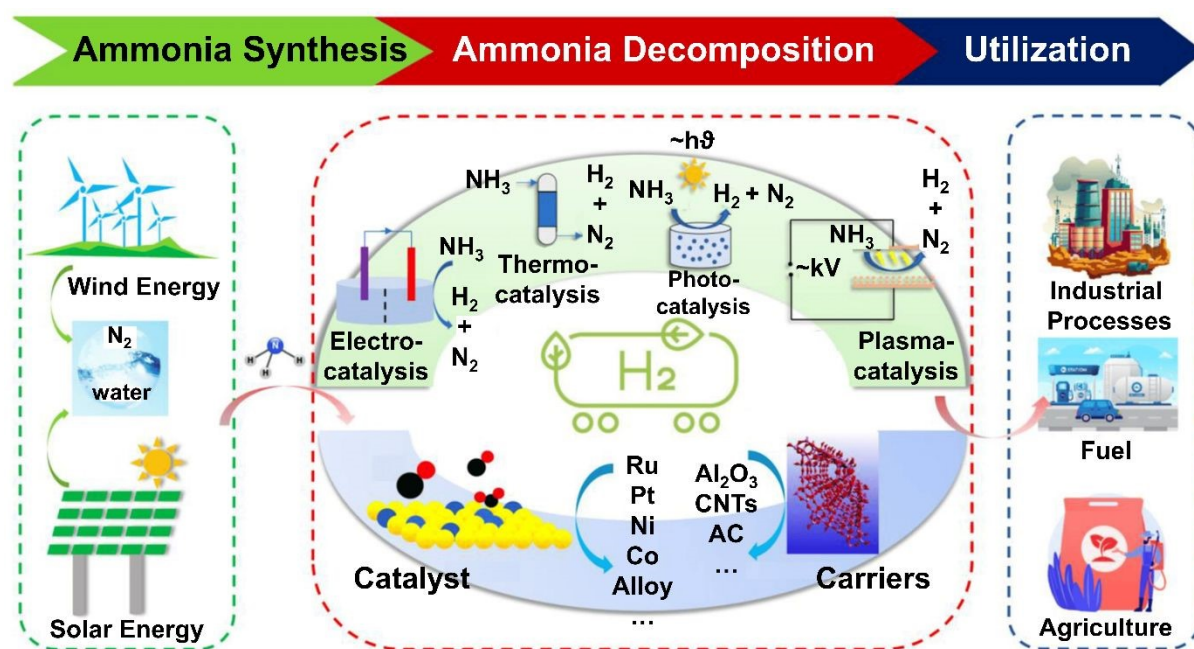
1

2 From this perspective, significant progress has been made in recent years in developing
 3 alternative methods, with a focus on reducing reaction temperatures. This advancement aims
 4 to lower energy consumption while enhancing hydrogen production efficiency⁵⁴. Until now,
 5 electric currents, electron beams, ions, microwaves, plasma, and solar energy are alternative
 6 approaches to provide new feasible solutions for ammonia decomposing (Fig. 1)⁵⁵. Although
 7 numerous reviews have been published on the progress of ammonia decomposition, the
 8 literature has overlooked assessing the different approaches for green H₂ generation from NH₃
 9 and the subsequent technical barriers to achieving a futuristic fuel and sustainable energy
 10 vector.

11 Hence, this review aims to summarize and analyze previously reported green ammonia
 12 cracking aspects, such as photocatalysis, electrocatalysis, and other approaches, as well as their



1 mechanisms of catalytic activity. Furthermore, the influences of recent revolution in data
 2 science, artificial intelligence (AI), and machine learning (ML), on the discovery of novel
 3 catalysts for the NH_3 -to- H_2 reaction are evaluated. Finally, based on the literature and our
 4 experience, the current challenges and future perspectives for achieving the rapid
 5 commercialization of NH_3 decomposition and green H_2 production are discussed.



7 **Figure 1.** The status of hydrogen generation from ammonia decomposition. This figure was
 8 adapted with the permission from Ref. ⁵⁶. Copyright 2023, MDPI.

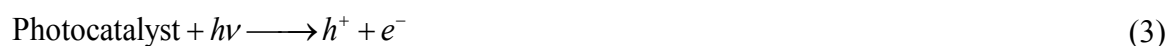
11 2. Photocatalysis

12 In recent decades, the study of photocatalytic ammonia decomposition reactions has garnered
 13 significant attention due to their potential applications in energy production, driven by growing
 14 concerns over environmental impact and the increasing demand for energy amid dwindling
 15 nonrenewable fossil fuel resources ¹⁹. The photocatalytic decomposition of NH_3 into N_2 and
 16 H_2 presents a viable approach, as it can be conducted at room temperature using recyclable
 17 catalysts and allows facile control of light exposure via a switch. Moreover, utilizing sunlight



1 for ammonia decomposition via photocatalysis represents an artificial photosynthetic reaction
2 that proceeds under alkaline conditions ⁵⁶.

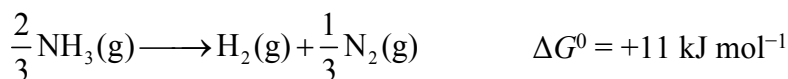
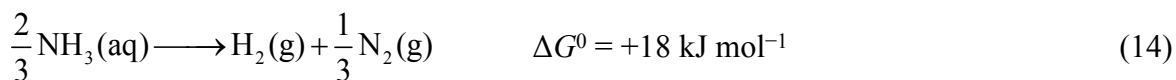
3 Fundamentally, photocatalysis involves a redox reaction that utilizes photogenerated electrons
4 (e^-) and holes (h^+) from semiconductors. The overall process unfolds in three key stages. First,
5 photons excite charge carriers, initiating the reaction. Next, these charges are separated and
6 migrate across the photocatalytic surface. Finally, the photo-activated charge carriers drive
7 catalytic reactions at the surface, facilitating water oxidation and reduction. These steps are
8 elaborated in Eqs. 3-12 ⁵⁷⁻⁶².



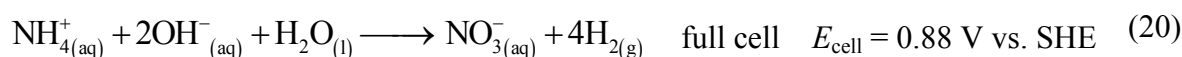
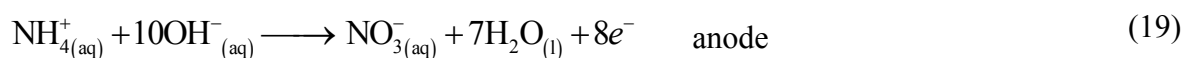
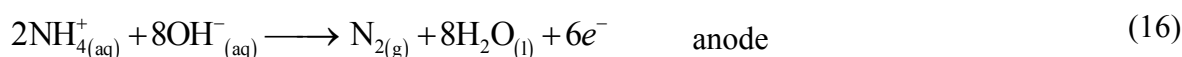
10
11 From a thermodynamic perspective, the production of hydrogen through the decomposition of
12 ammonia (Eqs. 13-14) is more favorable compared to splitting water ^{63, 64}.

13



View Article Online
DOI: 10.1039/D4CC06382A

1
2 Notably, photocatalytic reactions involving ammonia are feasible only when the reduction and
3 oxidation potentials of ammonia fall between the semiconductor's conduction band (CB) and
4 valence band (VB) potentials. During this process, various nitrogen-containing products such
5 as N_2 , NO_2^- , NO_3^- , and NO_x can be formed owing to their closely related redox potentials. The
6 specific potentials of these reactions are detailed in Eqs. 15-20⁶⁵ and Fig. 2a. Technically,
7 ammonia decomposition can yield varying quantities of different products depending on
8 several reaction parameters such as pH, temperature, initial ammonia or O_2 concentration, and
9 the presence of trapping or sacrificial agents. For an effective photocatalytic degradation of
10 ammonia, the photogenerated electrons and holes on the semiconductor surface must possess
11 appropriate reduction and oxidation capabilities. These enable reactions with species adsorbed
12 on the catalyst surface, such as O_2 , NH_4^+ , NO_2^- , and NO_3^- , facilitating the generation of free
13 radicals or diverse products.



1 Furthermore, the photocatalytic decomposition of ammonia typically ceases under acidic
2 conditions, suggesting that H^+ ions impede the transformation of ammonia into NH_2 free
3 radicals. As the pH increases, ammonia is likely to react with surrounding oxygen, forming
4 NO_2^- , NO_3^- , and other nitrogen oxides and adversely affecting hydrogen production. However,
5 many photocatalysts currently face significant challenges with carrier recombination and poor
6 light-harvesting efficiency. Consequently, the development of more effective photocatalytic
7 materials remains crucial for the advancement of ammonia treatment through photocatalytic
8 technologies ⁶⁶.

9 To date, only a group of photocatalysts, such as TiO_2 , ZnO , ZnS , Mo_2N , graphene, and their
10 metal-loaded hybrid materials, have been found effective in decomposing aqueous ammonia
11 solutions ⁵⁶. However, their hydrogen production rate, capped at $15.56 \mu\text{mol g}^{-1} \text{min}^{-1}$, remains
12 insufficient to satisfy practical application requirements ⁶⁷. To address this shortcoming,
13 Utsunomiya *et al.* ¹⁹ investigated the photocatalytic performance of Ni/TiO_2 catalysts in
14 ammonia decomposition and explored the mechanism of NH_3 breakdown by proposing three
15 distinct reaction pathways (Fig. 2b). These pathways involved the formation of N_2 and H_2
16 through intermediates radicals: route 1 entailed the formation of NH radicals via the removal
17 of one hydrogen atom from two NH_2 radicals; route 2 involved the direct coupling of adjacent
18 NH_2 radicals to form NH_2-NH_2 ; and route 2', where NH_2-NH_2 formation occurred through the
19 interaction of H_2N-NH_3 . The activation energies for routes 1 and 2 were determined to be 236
20 kcal mol^{-1} and $74.8 \text{kcal mol}^{-1}$, respectively, with route 2 being more energetically favorable.
21 Additionally, the pathways for N_2 and H_2 formation via NH_2-NH_2 coupling were further
22 delineated into route 2, which involved the coupling of NH_2 radicals to form H_2N-NH_2 , and
23 route 2', where NH_2 interacted with an NH_3 molecule in the gas phase.

24 Alternatively, beyond photocatalysis, solar heating catalysis demonstrates the highest
25 efficiency in sunlight utilization (approaching 100%) and can achieve temperatures up to 400



1 °C. This facilitates the heating of catalysts for thermocatalysis under natural solar irradiation.

2 In the context of solar-powered ammonia decomposition, cobalt-based catalysts are preferred

3 due to their abundance and effectiveness⁶⁷. Yuan *et al.*⁶⁷ developed a catalyst by immobilizing

4 single atoms of cobalt on cerium dioxide nanosheets (SA Co/CeO₂) (Figs. 2c and 2d) for

5 photocatalytic degradation of ammonia in tubular reactor at low temperatures (Fig. 2e). As can

6 be seen in Fig. 2f, integrated with a custom-built TiC/Cu-based solar heating device, the SA

7 Co/CeO₂ demonstrated a stable hydrogen generation rate of 2.7 mmol g⁻¹ min⁻¹ under 2 solar

8 irradiation, which is 572 times more effective than traditional weak sunlight-driven ammonia

9 decomposition. The hydrogen produced was found to be sufficiently pure to power a hydrogen

10 fuel cell without further purification directly. Theoretical calculations revealed that SA

11 Co/CeO₂ significantly lowers the energy barrier for nitrogen binding during ammonia

12 decomposition, thereby enhancing the reaction's progress (Fig. 2g).



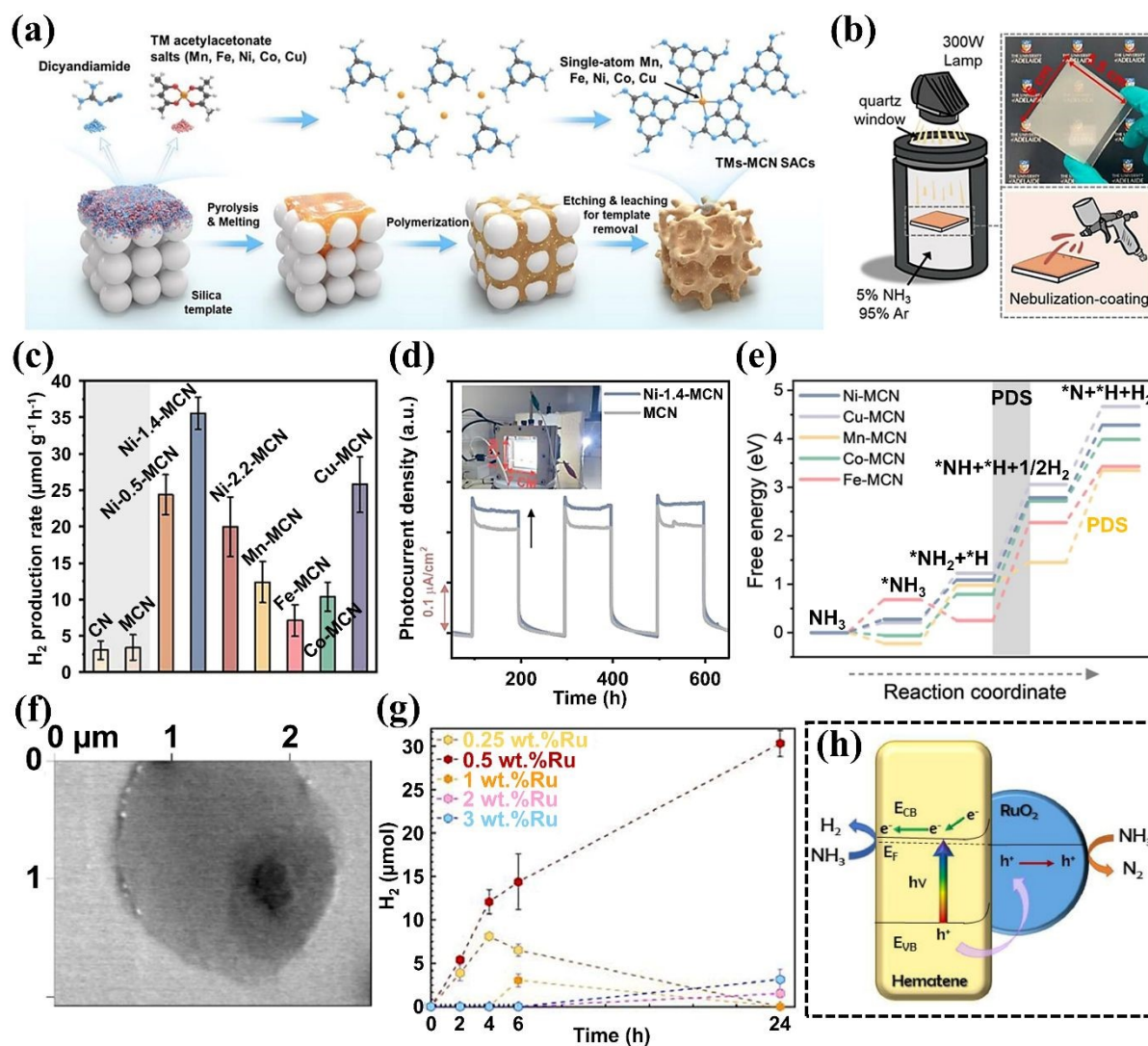
1 reaction mechanism for NH₃ decomposition to N₂ and H₂ on TiO₂ photocatalyst. This figure
2 was adapted with the permission of Ref. ¹⁹, Elsevier. (c) TEM image and (d) HAADF-STEM
3 image of SA Co/CeO₂. (e) Photograph of SA Co/CeO₂ loaded in a novel solar heating device
4 to drive hydrogen fuel cell under 2 solar irradiation. (f) H₂ production rate from NH₃
5 decomposition by SA Co/CeO₂. (g) Energy profiles for NH₃ decomposed as H₂ and N₂ on SA
6 Co/CeO₂ (111) and Co (111) surfaces. These figures were adapted with the permission of Ref.
7 ⁶⁷. Copyright 2023, Elsevier.

8
9 Moreover, Lin *et al.* ⁶⁹ employed a straightforward nebulization-coating technique to
10 immobilize a wide array of single-atom transition metals (TMs: Co, Mn, Fe, Ni, Cu) onto
11 microporous carbon nitride (MCN) (Fig. 3a), creating catalyst panels designed for solar-light-
12 driven photocatalytic gaseous ammonia splitting (Fig. 3b). Under ambient conditions, the
13 optimized Ni-MCN demonstrated a hydrogen production rate of 35.6 μmol g⁻¹ h⁻¹,
14 significantly outperforming pure MCN (by approximately 14-fold) and other composite
15 alternatives (Fig. 3c). This enhanced photocatalytic activity and photocurrent response (Fig.
16 3d) can be attributed to the presence of Ni-N₄ sites, which enhance the optical properties,
17 expedite charge carrier separation/transfer, and improve the kinetics of ammonia splitting on
18 the catalysts. Regarding Fig. 3e, the Ni site on MCN is the most favorable for NH₃ splitting
19 among all these TMs due to its lowest free energy increase in the potential-determined step
20 (PDS).

21 In another study, Dzibelov'a *et al.* ⁷⁰ utilized an ultrasound-supported exfoliation technique to
22 anchor ruthenium oxide nanoparticles onto 2D hematene (α -Fe₂O₃) (Fig. 3f) for the
23 decomposition of an aqueous ammonia solution into hydrogen and nitrogen under visible light
24 irradiation. Experimental results demonstrated that with an optimal ruthenium dosage of 0.5
25 wt%, the Ru-hematite, after 24 hours, achieved a hydrogen yield that was 2.5 times higher than



1 that of pure hematene (Fig. 3g), attributed to the enhanced generation of electrons and holes
 2 (Fig. 3h). Moreover, without any cleaning interventions, the Ru-hematite photocatalyst
 3 exhibited only an 11% reduction in photocatalytic activity after five consecutive runs,
 4 suggesting its suitability for practical applications.



6
 7 **Figure 3.** (a) Schematic of the synthesis procedure of TMs-MCN SACs. (b) Illustration of the
 8 reaction system and nebulization-coating method for fabricating TMs-MCN panels. (c) Rates
 9 of H₂ production by CN, MCN, and Ni-MCNs with different Ni loadings and TMs MCNs (TMs
 10 = Mn, Fe, Co, Ni, Cu, with a similar loading percentage of ~1.4 wt %). (d) Photocurrent
 11 responses of MCN and Ni-1.4-MCN (inset: picture of the large-sized cell). (e) Energy profiles



1 for the reaction process. These figures were adapted with the permission of Ref. ⁶⁹ Copyright
 2 2023, American Chemical Society. (f) Correlative probe and electron microscopy image of
 3 hematene sheet. (g) Decomposition of ammonia over Ru-hematene samples to optimize weight
 4 loading of Ru. (h) Schematic mechanism of ammonia decomposition by Ru-hematene
 5 photocatalyst. These figures were adapted with the permission of Ref. ⁷⁰. Copyright 2023,
 6 Elsevier.

8 3. Electrocatalysis

9 Recently, hydrogen generation through electrochemical reactions, such as ammonia
 10 decomposition by electrocatalysis at moderate temperatures, has attracted more attention.⁷¹
 11 However, ammonia decomposition faces challenges such as high overpotentials, unfavorable
 12 thermodynamics, and slow reaction kinetics ⁷². Based on the different existing states of NH₃,
 13 electrochemical ammonia decomposition can be categorized into the electrolysis of (i) aqueous
 14 ammonia solution, or (ii) liquid ammonia. In the electrolysis of alkaline aqueous ammonia
 15 solutions, NH₃ undergoes oxidation in the existence of OH⁻ ions at the anode (Eq. 21) ⁷³,
 16 whereas H₂O can be reduced at the cathode (Eqs. 22 and 23) ^{71, 74, 75}.

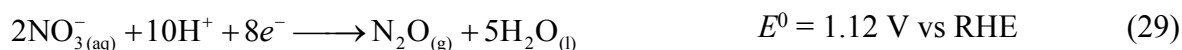
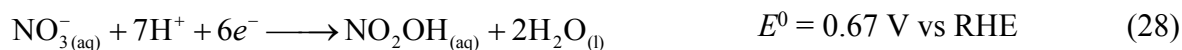


18
 19 In 2002, Zisekas *et al.* ⁹ utilized silver as the reactor electrode to conduct the first tests on
 20 hydrogen production via electrocatalytic decomposition of ammonia. These tests demonstrated
 21 that NH₃ conversion efficiency ranged between 25–35% at temperatures of 773–873K,
 22 indicating that reactor temperatures remained relatively high. It is well accepted that the energy



1 density of hydrogen in liquid ammonia [$\text{NH}_3(\text{l})$, 3.6 kW h L^{-1}] is significantly higher compared
 2 to that in alkaline aqueous ammonia solution [$\text{NH}_3(\text{aq})$, 1.0 M , 0.1 kW h L^{-1}]. Fundamentally,
 3 the electrolysis of liquid ammonia differs from that of aqueous ammonia solutions, as both the
 4 anodic and cathodic half-reactions in liquid ammonia avoid the excessive oxidation of
 5 ammonia that typically occurs in the presence of water ⁷¹. Furthermore, the gravimetric
 6 H_2 density is as low as 6.1 mass % according to its solubility to water, 34.2 mass % at 20°C
 7 ⁷⁶. Thus, Hanada *et al.* ⁷⁷ evaluated the direct electrolysis of liquid ammonia, where alkaline
 8 metal amides (MNH_2 , $\text{M} = \text{Li, Na, K}$) were utilized as the supporting electrolyte. Amides such
 9 as LiNH_2 , NaNH_2 , KNH_2 , and $\text{N, N-dimethylformamide}$ have enabled the electrolysis of liquid
 10 ammonia. This process was conducted at exceptionally low temperatures, ranging from -70 to
 11 -65°C , using pure platinum electrodes ⁷⁸.
 12 Moreover, during electrocatalytic reaction, NH_3 can be converted aqueous to NO_3^- and then to
 13 products such as HNO_2 , NO , NH_2OH , NH_3 , N_2O , and N_2 (Eqs. 24-30). Generated nitrogen is
 14 benign and easily separable, and is the most stable nitrate reduction product with a standard
 15 redox potential (E^0) of 1.25 V vs. RHE ⁷².

16



17



1 Technically, the electrocatalytic decomposition of ammonia encompasses two primary phases
2 (i) the ammonia oxidation reaction (AOR) and (ii) the hydrogen evolution reaction (HER). An
3 effective high-efficiency electrocatalyst should be capable of catalyzing both AOR and HER
4 at a low potential ³⁶. Despite its potential, the activity level of AOR is insufficient for low-
5 temperature operations. AOR integrates more easily with fuel cell technologies and provides a
6 more effective method for hydrogen generation than water electrolysis, which represents the
7 second most common hydrogen production method and accounts for approximately 4% of
8 global hydrogen production. Water electrolysis, which is not thermodynamically favored,
9 theoretically necessitates applying a voltage as high as 1.23 V to break down highly stable
10 water molecules, requiring about 180 MJ of energy to produce 1 kg of H₂. In contrast, AOR
11 has a significantly lower energy requirement of approximately 33 MJ per kg of hydrogen
12 generated ⁷⁹.

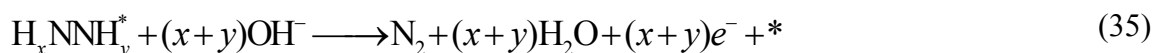
13 Research has demonstrated that the electrocatalytic activity for ammonia oxidation correlates
14 with the properties of surface materials. The catalyst remains active when intermediate NH_x
15 species are present but becomes inhibited when strongly binding nitrogen species are formed
16 ⁸⁰. In this context, the widely accepted mechanism was proposed by Gerischer and Mauerer in
17 1970, with the fundamental steps detailed in Eqs. 31-35. Briefly, NH₃ can be deprotonated in
18 the presence of hydroxyl ions in Eqs. 31-33, producing water molecules while simultaneously
19 releasing an electron at each step. N* adatoms (formed in Eq. 33) are surface poisons because
20 of a typically large kinetic barrier for N–N bond formation and release nitrogen. Thus, adsorbed
21 NH_x (and NH_y) species can interact with one another to form an N–N bond, subsequently
22 generating an H_xNNH_y species (Eq. 34). Regarding the Gerischer–Mauerer mechanism, these
23 species are then deprotonated to N₂, which desorbs from the surface; however, the identity of
24 the NH_x and NH_y species that react to form the N–N bond remains in dispute (Eq. 35) ⁸¹.

25





(31) View Article Online
DOI: 10.1039/D4CC06382A



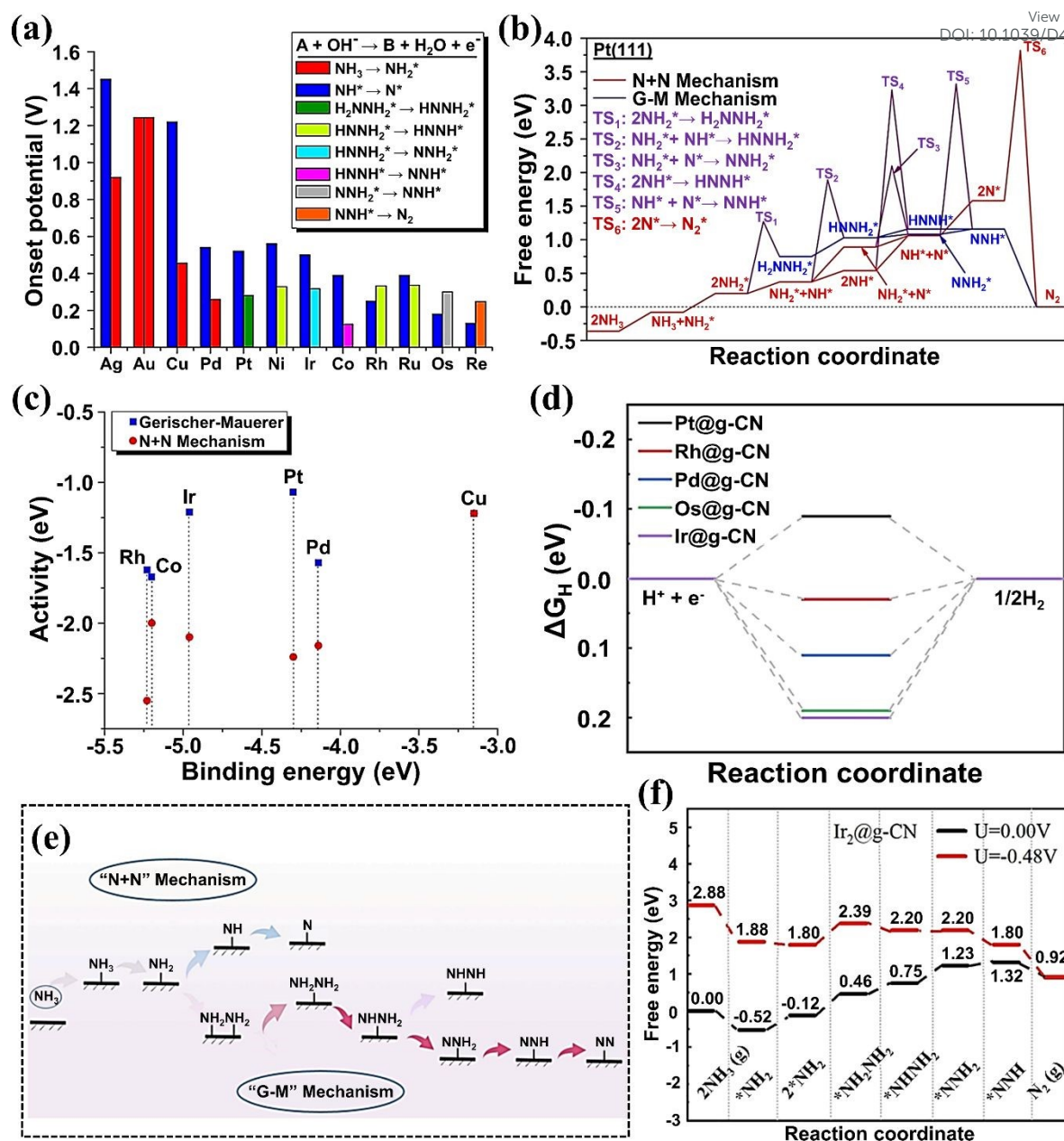
1
 2 The catalytic activity can be substantially enhanced when a portion of the metal is utilized as
 3 an electrode by applying a current or potential between the catalyst and a counter electrode
 4 deposited on the solid electrolyte³⁶. To date, a diverse range of materials, such as noble metals,
 5 metal oxides, and non-metals, have demonstrated high catalytic activity for ammonia electro-
 6 oxidation. Notably, Pt has emerged as the most effective electrocatalyst for this reaction.
 7 However, most ammonia electro-oxidation systems necessitate strong alkaline media (such as
 8 NaOH), leading to rapid deactivation and poisoning of Pt catalysts, as well as oxygen evolution
 9 and NO_x production. Under strongly alkaline conditions, electrodeposited Pt electrodes and
 10 nanotubes have effectively oxidized ammonia into hydrogen⁷⁸.
 11 In this context, Herron *et al.*⁸¹ examined AOR efficiency on various face-centered cubic (fcc)
 12 metals (Au, Ag, Cu, Pd, Pt, Ni, Ir, Co, Rh, Ru, Os, and Re) using density functional theory
 13 (DFT) calculations. They reported that Pt exhibited the most promising catalytic activity,
 14 followed by Ir and Cu, due to its low onset potential (Figs. 4a and 4b). It was found that
 15 adsorbed NH₂ was the dominant intermediate, facilitating the preferred N–N bond formation
 16 both kinetically and thermodynamically (Fig. 4c). In another study, Zhong *et al.*⁸⁰ investigated
 17 catalytic electro-oxidation of liquid ammonia using transition metal dimers (Fe₂, Co₂, Ru₂, Rh₂,
 18 and Ir₂) anchored on graphite-carbon nitride monolayers (TM₂@g-CN). Their findings
 19 reinforce the mechanism proposed by Gerischer and Mauerer, where N–N bond formation is



1 facilitated by hydrogenated NH_x species rather than N adatoms (Fig. 4d). Catalytic activity
2 studies demonstrated that Fe, Co, Ru, Rh, and Ir anchored in g-CN monolayers are
3 exceptionally promising AOR catalysts due to their low limiting potentials of -0.47 , -0.5 ,
4 -0.48 , -0.52 , and -0.48 V, respectively. Among them, $\text{Ir}_2@\text{g-CN}$, as a bifunctional catalyst
5 for electrocatalytic NH_3 decomposition, showed low energy barriers of 0.48 eV and 0.20 eV
6 for AOR (Fig. 4e) and HER (Fig. 4f), respectively. It was found that modulating TM atoms
7 with varying d-electron numbers allows for tuning the d -band center (ϵ_d) of TM atoms on
8 $\text{TM}_2@\text{g-CN}$, providing a predictive measure for AOR performance and offering theoretical
9 guidance for designing advanced AOR electrocatalysts.

View Article Online
DOI: 10.1039/D4CC06382A





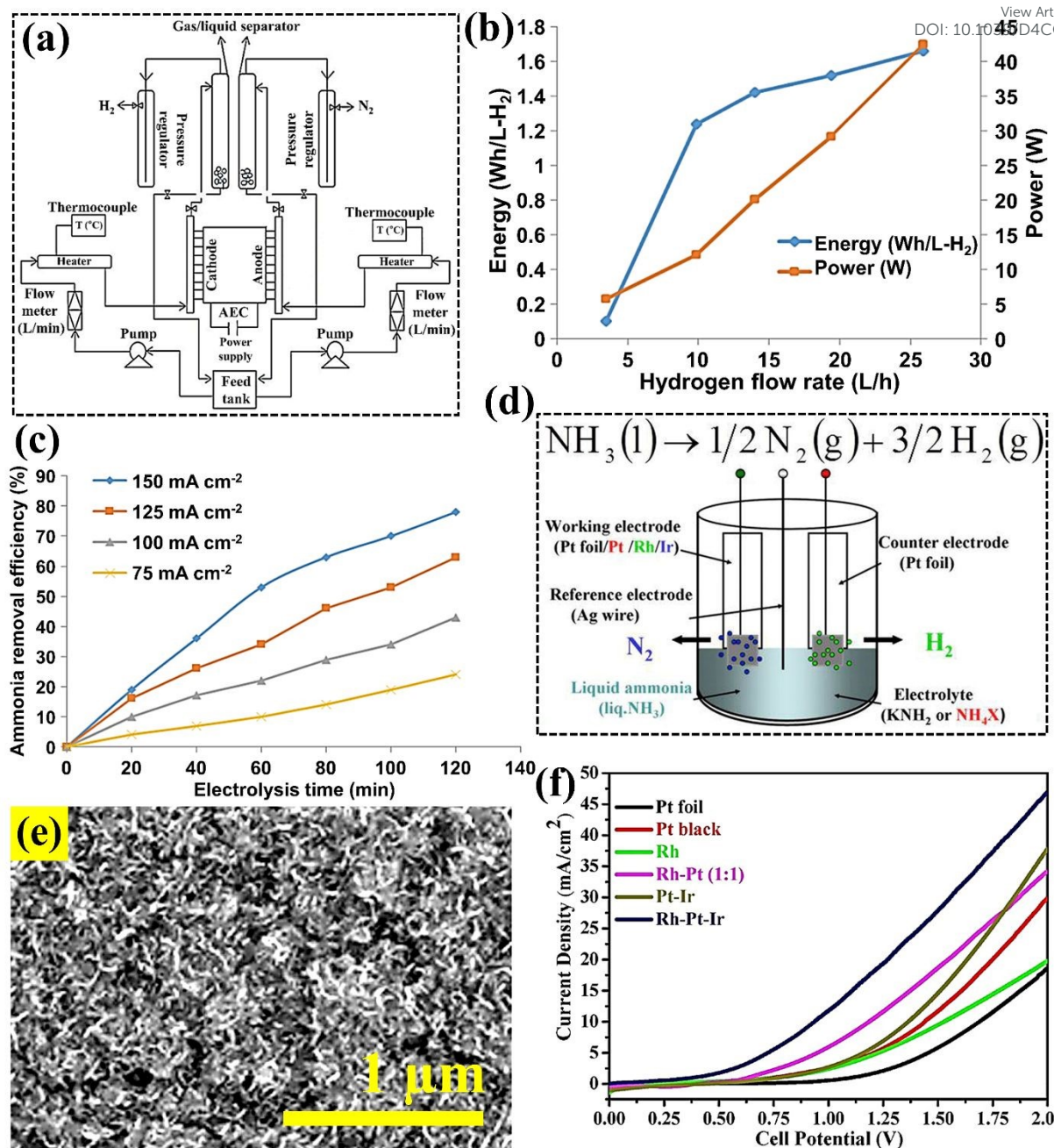
1
2 **Figure 4.** (a) Estimated onset potential for close-packed facets of transition metals. (b) Activity
3 as predicted by Sabatier analysis for both mechanisms at 0 V_{RHE} . (c) Free-energy diagram for
4 ammonia electro-oxidation on Pt(111) at 0 V_{RHE} . These figures were adapted with the
5 permission of Ref. ⁸¹. Copyright 2015, American Chemical Society. (d) Proposed mechanism
6 for AOR on $\text{TM}_2\text{@g-CN}$. (e) The calculation free energy diagram of AOR through the
7 Gerischer–Mauerer mechanism on Ir₂@g-CN at different applied potentials. (f) The calculated



1 free energy diagram of the HER on $\text{TM}_2\text{@g-CN}$ samples. These figures were adapted with the View Article Online
DOI: 10.1039/D4CC06382A
2 permission of Ref. ⁸⁰. Copyright 2023, Elsevier.

3
4 In Modisha's study ⁸², decomposition of ammonia using a Pt-Ir electrocatalyst was investigated
5 in a potassium hydroxide (KOH, 5M) solution (Fig. 5a). This research demonstrated that the
6 current density of ammonia electro-oxidation reaction rose at high temperature and ammonia
7 concentration, achieving a peak ammonia conversion of 78% at 2300 ppm (Fig. 5b). From Fig.
8 5c, the highest hydrogen flow rate recorded was 25 L h⁻¹, with an associated energy
9 consumption of 1.6 Wh L⁻¹ H₂⁻¹. The purity of hydrogen, as determined by gas
10 chromatography, was found to be 86%. Moreover, Dong *et al.* ⁸³ synthesized five types of
11 electrocatalysts, including Pt-Black, Rh, Pt-Ir, Rh-Pt, and Rh-Pt-Ir alloys, aimed at reducing
12 the overpotential of the anode reaction for ammonia cracking (Fig. 5d). These alloys were
13 electrochemically evaluated for their efficacy in ammonia decomposition in the presence of
14 NH₄Cl. The trimetallic Rh-Pt-Ir and the bimetallic Pt-Ir, as well as the Rh-contained alloy
15 electrodes, demonstrated enhanced activity and reduced deactivation. Notably, the Rh-Pt-Ir
16 alloy anode (Fig. 5e) exhibited the highest electrocatalytic activity, achieving the lowest
17 minimum potential (E_{min}) of approximately 0.47 V and the highest current density of 46.9 mA
18 cm⁻² at 2.0 V (Fig. 5f). The results of this research reflect that the energy required for hydrogen
19 generation from the electrolysis of liquid NH₃ can be significantly lowered through strategic
20 selection and compositional optimization of alloy catalysts.





1
2 **Figure 5.** (a) Schematic representation of ammonia electrolysis process for hydrogen
3 production. (b) Volumetric hydrogen generation rates and corresponding required energy and
4 power input (cell retention time (Rt): was 12.5 min, 2000 ppm NH_3 in 5 M KOH at 55 $^{\circ}C$). (c)
5 Ammonia decomposition efficiency as a function of time and current density. These figures
6 were adapted with the permission of Ref. ⁸². Copyright 2016, Elsevier. (d) Schematic
7 electrolysis of liquid ammonia using different ammonium salt electrolytes with the reference
8 electrode. (e) SEM image of the freshly prepared Rh-Pt-Ir electrocatalyst. (f) Cyclic

1 voltammetry curves of NH_3 (l) with 1 M NH_4Cl in two-electrode system. These figures were
2 adapted with the permission of Ref. ⁸³. Copyright 2016, Elsevier.

3

4 **4. Plasma**

5 As mentioned earlier, significant research efforts have been directed toward developing
6 alternative energy supply methods for ammonia decomposition. These methods include the use
7 of electric currents ⁸⁴, electron beams ⁸⁵, microwaves ⁸⁶, and plasma ⁸⁷, which offer higher
8 conversion rates at lower temperatures compared to traditional thermal catalysis. Among them,
9 there has been a notable shift towards exploring non-thermal plasma (NTP) for catalytic
10 ammonia decomposition at low temperatures. This approach potentially enhances the response
11 time and modularity of ammonia-based hydrogen production systems, thereby improving their
12 applicability in sectors like transportation ⁸⁸.

13 Plasma is generally defined as a state of gas where the atoms are partially or fully ionized,
14 maintaining overall electrical neutrality, containing a large number of highly energetic
15 electrons and reactive species (e.g., excited molecules, atoms, ions, and radicles) (Figs. 6a-6c)
16 ^{9, 89, 90}. It was found that integrating non-thermal plasma with a catalyst can significantly modify
17 the catalytic reaction pathway, leading to enhanced selectivity or reaction rates through the
18 interaction of plasma, reactant, and catalyst ⁸⁹. Notably, the H_2 energy yield from the plasma
19 catalysis method is nearly five times greater than that achieved through thermal catalysis. This
20 indicates that plasma catalysis substantially enhances the economic efficiency of hydrogen
21 production from ammonia ⁹. In 2006, research on the impact of dielectric barrier discharge
22 plasma on ammonia decomposition revealed that using a commercially available bulk Fe-based
23 catalyst significantly increased NH_3 conversion rates. Specifically, NH_3 conversion escalated
24 from 7.4% to 99.9% when the Fe-based catalyst was positioned within a plasma zone at 410
25 $^\circ\text{C}$ ⁹¹. In this context, the researchers further optimized the ammonia decomposition process by



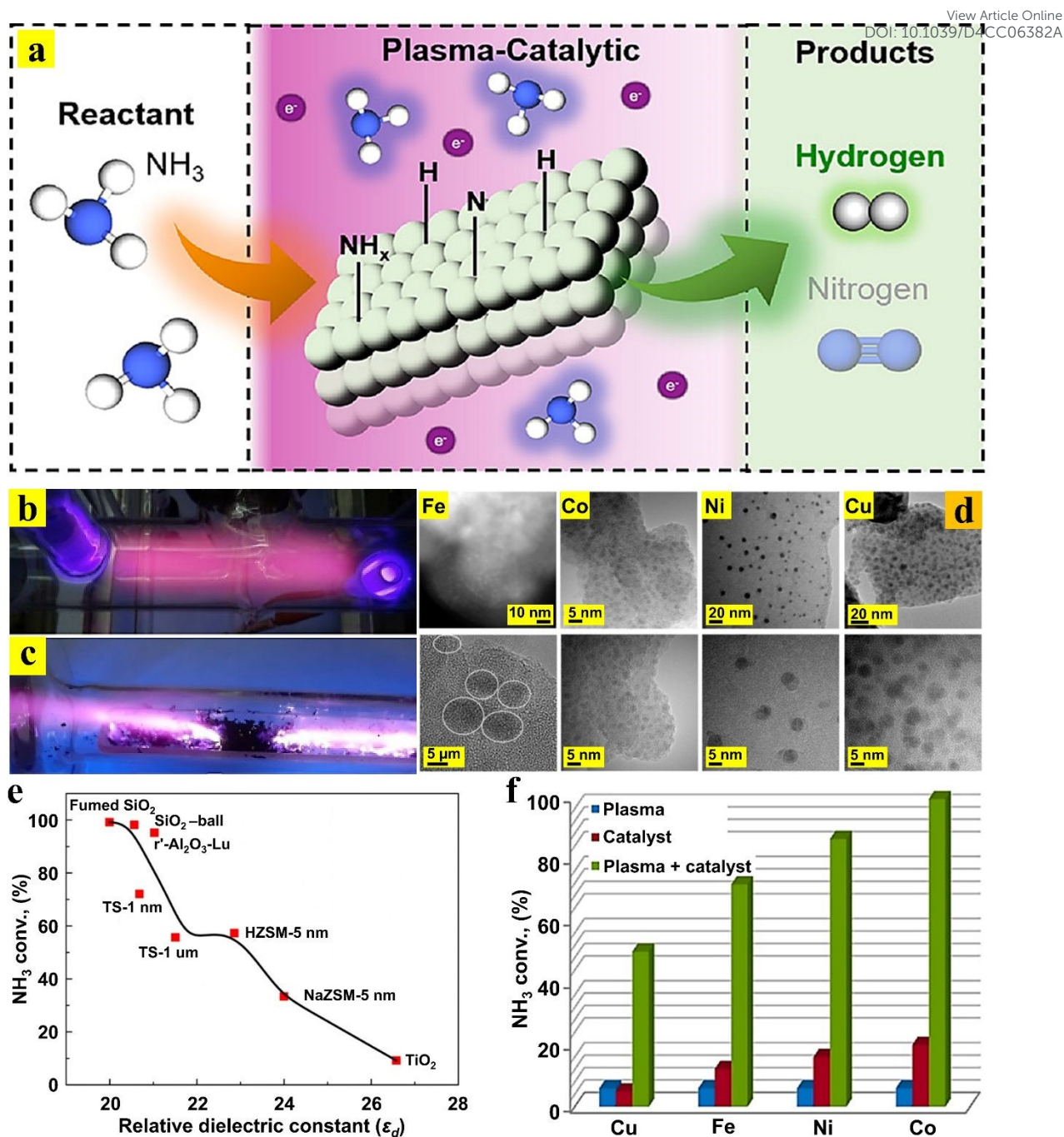
1 utilizing low-temperature plasma, either using high-performance catalysts or by identifying
2 optimal reaction conditions.

3 In 2015, Wang *et al.*⁹¹ conducted a comparative study on the efficiencies of hydrogen
4 generation from ammonia using both thermal and plasma catalysis methods over different low-
5 cost metal catalysts (Fe, Co, Ni, Cu) on fumed SiO₂ support (Fig. 6d). The results indicated
6 that the NH₃ conversion strongly depends on the metal–N bond strengths and on the relative
7 dielectric constant of the support in the plasma reaction. It was observed that the moderately
8 strong Co–N bonds can be expected to improve the plasma–catalyst synergy, thus leading to
9 higher NH₃ conversions (Fig. 6e). Notably, the relative dielectric constant (ϵ_d) of the support
10 can efficiently contribute to plasma-catalytic NH₃ decomposition performance. As shown in
11 Fig. 6f, a support with a small ϵ_d facilitates plasma-catalytic ammonia decomposition.
12 Technically, plasma gas discharge can rapidly heat the reaction/catalyst, enhancing the energy
13 efficiency of hydrogen production. Additionally, plasma has been shown to facilitate the rate-
14 limiting step by accelerating the recombinative desorption of N_{ad} from the catalyst bulk
15 structure⁸⁹. In another study, the effects of varying discharge zone lengths on the efficiency of
16 plasma-catalytic ammonia decomposition at a set discharge frequency were investigated. The
17 research revealed that doubling the discharge zone length from 3.0 cm to 3.5 cm at a frequency
18 of 10 kHz resulted in a twofold increase in NH₃ conversion efficiency⁹. Consequently, these
19 findings indicate that non-thermal plasma and catalysts can synergistically interact to
20 efficiently convert NH₃ to H₂ under mild conditions. However, despite the potential of plasma-
21 catalytic processes, the number of catalysts tested and evaluated remains limited compared to
22 those used in thermocatalysis.

23 Tables 2–4 summarize the literature on hydrogen generation from ammonia cracking through
24 photocatalytic, electrocatalytic, and plasma processes, respectively.

25





1
2 **Figure 6.** (a) Schematic presentation for the plasma-catalytic NH_3 decomposition. This figure
3 was adapted with the permission of Ref. ⁹². Copyright 2024, American Chemical Society. In
4 situ plasma-assisted catalytic NH_3 conversion system (b) under NTP conditions and (c) glow
5 discharge reactor. These figures were adapted with the permission of Ref. ⁹³. Copyright 2022,
6 MDPI. (d) TEM micrographs of Fe, Co, Ni, and Cu catalysts supported on fumed SiO_2 (reduced
7 in H_2 plasma). (e) NH_3 conversions on Co catalysts on various supports as a function of relative



1 dielectric constants of supports in plasma + catalyst mode (NH_3 feed 40 mL min^{-1} , temperature
2 $450 \text{ }^\circ\text{C}$, supported catalyst 0.88 g , discharge gap 3 mm , discharge frequency 12 kHz). Influence
3 of metals on NH_3 conversion in plasma + catalyst, plasma, and catalyst modes (similar
4 condition for 3b). These figures were adapted with the permission of Ref. ⁹². Copyright 2024,
5 American Chemical Society.

6
7 **Table 2.** Performance comparison of different catalysts toward photocatalytic NH_3
8 decomposition.

Photocatalyst	Light source	Time	Initial NH_3 concentration	Maximum decomposition ability	Ref.
Pt–TiO ₂ (0.5 wt% Pt)	450 W high pressure Hg lamp	24 h	5 mM	Over 95%	94
Ni/TiO ₂ (0.5 wt% Ni)	500 W Xe lamp	3 h	5 mL, 0.59 mol L^{-1}	131.7 $\mu\text{mol H}_2$ per g- catalyst	19
Ce-doped TiO ₂ (1.4 wt% Ce)	8 W Hg pen-ray lamp	10 h	100 mL, 0.8274 g L^{-1}	1010 mmol H_2 per g- catalyst	95
N–C@TiO ₂	25 W UV lamp	5 min	100 μL aqueous ammonia (30%)	100%	96
MoS ₂ @TiO ₂	25 W UV lamp	7 min	100 μL aqueous ammonia (30%)	91%	97
MoS ₂ /N-doped graphene	300 W UV-visible lamp	8 h	100.0 mg L^{-1}	99.6%	98
Nitrogen-doped rGO/TiO ₂	8 W Hg pen-ray lamp	12 h	0.883 g L^{-1}	$208 \mu\text{mol h}^{-1} \text{ g}^{-1}$	78
GQDs (graphene quantum dots)/CN (g-C ₃ N ₄)	150 W Xe arc lamp	7 h	1.5 mg L^{-1}	90%	99
ZnO/Ag	300 W Xe lamp	2.5 h	1.5 mg L^{-1}	Circa 90%	100

9

10



1 **Table 3.** Performance comparison of different catalysts toward electrocatalytic NH_3
 2 decomposition.

Catalyst	Catalyst loading (mg cm^{-2})	Electrolyte	Onset potential	Current density (mA cm^{-2})	Scan rate (mV s^{-2})	Ref.
PtIr/C	2.00	1.0 M NH_3	0.470 V_{RHE}	–	10	101
RGO/Pt-Ir	–	1.0 M NH_4OH	–0.400 $V_{\text{Ag}/\text{AgCl}}$	20.00 at 0 $V_{\text{Ag}/\text{AgCl}}$	10	102
Pt ₉₀ Ru ₁₀ /C	1.00	1.0 M NH_4OH + 1.0 M KOH	–	0.920 at –0.210 $V_{\text{Hg}/\text{HgO}}$	20	103
Pt _x Ir _{100-x} /MgO	–	0.1 M NH_3 + 0.2 M NaOH	0.530 V_{RHE}	1.00 at 0.710 V_{RHE}	20	104
SnO ₂ -Pt/C	0.028	0.1 M NH_3 + 0.1 M KOH	0.450 V_{RHE}	1.62 at 0.690 V_{RHE}	20	53

3

4 **Table 4.** Performance comparison of different catalysts toward plasma-assisted catalytic NH_3
 5 decomposition.

Catalyst	Power	Reactor configuration	Temperature ($^{\circ}\text{C}$)	Pressure (bar)	Catalyst amount (g)	NH_3 flow rate (L min^{-1})	NH_3 conversion rate (%)	Ref.
FeO	12 kHz 26 W	DBD ^a reactor	410	–	10	0.04	> 99.9	105
Ni- Al_2O_3	23.8 kHz 0–700 W	Non-thermal arc reactor	400–843	–	200	30.00	–	106
Ru- Al_2O_3	10 kHz 12–20 kV	DBD reactor	–	1	–	0.10–1.00	85.7	107
Metal-Mg Al_2O_4	1.0–3.5 kHz 10–25 W	DBD reactor	–	1	–	1.00	82.0	108
No catalyst	10 kHz 3.5–22 kV	DBD reactor	–	–	–	0.50	13.0	109

6 Note: ^a dielectric barrier discharge.

7



1 5. Other

2 It is well accepted that the alternative methods for ammonia decomposition, such as
3 electrocatalysis and photocatalysis, often depend on complex catalysts that include costly
4 precious metals. While non-precious metals are more affordable, they tend to exhibit lower
5 catalytic efficiencies and reduced stabilities ¹¹⁰. To tackle the challenges in conversion
6 performance, recently, ammonia-water has been recognized as a promising liquid hydrogen
7 carrier with the potential for widespread use in hydrogen generation. However, the hydrogen
8 derived from ammonia-water still poses main challenges. Despite advancements in various
9 methods to enhance the efficiency of hydrogen production from ammonia-water, these
10 techniques have yet to reach a level that is suitable for practical industrial applications ¹¹⁰. In
11 this context, Yan *et al.* ¹¹⁰ developed a novel, eco-friendly, and ultrafast method for extracting
12 hydrogen from ammonia-water without a catalyst and under ambient conditions using the laser
13 bubbling in liquids (LBL) approach. This technique is entirely different from conventional
14 catalytic methods for hydrogen extraction from ammonia-water. The LBL involves a focused
15 pulsed laser directly beneath the surface of the liquid. When the pulsed laser is applied to
16 ammonia-water, the molecules can be rapidly excited and ionized. This process generates
17 cavitation bubbles at the focus point that achieve transient high temperatures, creating an
18 optimal microspace for efficient hydrogen extraction. It was reported that the real adequate
19 time of laser action on ammonia-water was just 0.36 ms per hour and the actual hydrogen yield
20 reached 93.6 mol h⁻¹ at laser “light-on” time, reflecting the acceptable efficiency of the LBL
21 process.

22 Another attempt to develop a new approach toward ammonia decomposition was performed
23 by McLennan and Greenwood ¹¹¹, discovering that electric discharge in a cathode ray tube can
24 rapidly decompose ammonia. By eliminating the electric current, they focused on the
25 decomposition using only high-speed electron beams, achieving up to 30% decomposition with



1 pure ammonia. They also examined the effects of the presence of high-speed electrons (electron
2 spark) on the reaction rate, noting ammonia dilution with N₂ enhanced the reaction while H₂
3 inhibited it. Similarly, Hirabayashi and Ichihashi ¹¹² explored ammonia decomposition using
4 ion beams on various catalysts, identifying vanadium and niobium nitrides (V_nN_m⁺ and
5 Nb_nN_m⁺ ($n = 3-6$; $m = n, n-1$)) as promising for hydrogen production.

7 **6. Predicting NH₃ decomposition efficiency by machine learning**

8 It is well recognized that the broad temperature range of the ammonia decomposition process
9 in practical applications makes it difficult to monitor catalyst changes during the reaction,
10 which is also a major barrier to its practical implementation ¹¹³. In addition, discovery of
11 catalysts for NH₃ decomposition is a crucial aspect and has traditionally relied on trial-and-
12 error experiments ¹¹³⁻¹¹⁵. Therefore, utilizing DFT and numerical modeling techniques can
13 significantly accelerate research by validating the fundamental mechanisms of ammonia
14 decomposition ³⁴.

15 In recent decades, machine learning (ML) technology has emerged as a powerful tool in
16 designing novel catalysts, understanding composition-structure-property relationships, and
17 analyzing complex data patterns. This efficient computational approach streamlines
18 thermocatalytic ammonia decomposition while minimizing the need for extensive human and
19 material resources in catalyst design ¹¹³. The strength of ML algorithms lies in their capacity
20 to learn from historical data without the need for explicit programming. This approach is
21 anticipated to demonstrate high fidelity in identifying optimal operating conditions, not only
22 for NH₃ cracking in the gas phase but also for optimizing CO₂ capture, hydrocracking, and
23 dimethyl ether synthesis ¹¹⁶.

24 To date, several studies have utilized ML models to identify and optimize catalysts for
25 ammonia decomposition. For instance, Williams *et al.* ¹¹⁷ assessed the integration of ML with



1 high-throughput experimentation to optimize catalyst compositions with low ruthenium
2 content for NH₃ decomposition in a 16-channel parallel reactor system. Their model was
3 developed by training in three progressive stages, utilizing datasets of 3, 22, and 28 catalysts.
4 By analyzing the chemical properties of the secondary metal and reaction temperature, the
5 model effectively predicted ammonia decomposition efficiency. It was found that by
6 employing the random forest algorithm enabled catalyst performance predictions with a mean
7 absolute error of less than 0.16, demonstrating the approach's accuracy and reliability. In
8 another study, Guo *et al.*¹¹³ utilized ML using random forest regression, support vector
9 machines, and gradient boost regression approaches, to statistically analyze ammonia
10 decomposition as a function of catalyst properties and reaction conditions. Their findings
11 revealed a strong positive correlation between catalytic efficiency and reaction temperature,
12 with the gas hourly space velocity (GHSV) emerging as a key factor influencing both ammonia
13 conversion and hydrogen production rates. Notably, optimal decomposition and hydrogen
14 formation were achieved with a total metal loading below 20%wt. It was concluded that among
15 the models tested, the gradient boost regression tree demonstrated strong predictive accuracy,
16 achieving an R^2 greater than 0.85, an RMSE below 13.24, and an MAE under 10.31.
17 Although ML has shown promising results, developed models often tend to be case-specific,
18 limiting their generalizability across different catalyst systems. In addition, traditional ML-
19 guided catalyst screening can be challenging to obtain in new catalytic systems, specifically
20 molecular catalysts for AOR electrocatalysts¹¹⁸. To address these theoretical limitations, recent
21 studies aim to develop an ML model specifically designed to accurately predict the conversion
22 of NH₃ to H₂. By compiling data from published literature, an extensive experimental database
23 was established, and the relationship between independent variables and dependent responses
24 was thoroughly evaluated using statistical analyses and mechanistic insights¹¹³.



1 Moreover, integrating reaction kinetics into ML framework presents a promising research
2 direction. In this context, understanding the role of reaction kinetics in predicting H₂ formation
3 rates during NH₃ decomposition can provide valuable insights into catalyst behavior and
4 improve predictive accuracy. Additionally, incorporating hydrogen inhibition effects into the
5 ML model will enable researchers to better capture catalyst dynamics, ultimately enhancing
6 performance predictions ¹¹³. Notably, the exploration of advanced ML techniques can offer
7 new insights into developing the connections among the characteristics of substances and their
8 catalytic activity, selectivity, and stability of the complex catalytic systems ¹¹⁹. In the future,
9 with further research and widespread application of artificial intelligence technologies,
10 ammonia decomposition processes are expected to become more efficient and environmentally
11 sustainable, offering robust support for sustainable development.

13 **7. Further challenges for ammonia decomposition**

14 Extensive research has focused on developing highly active and durable catalysts for ammonia
15 decomposition at minimal temperatures, intending to further lower the temperature to improve
16 efficiency and promote environmentally sustainable processes. It is widely recognized that
17 support for NH₃ decomposition catalysts should exhibit high basicity alongside high
18 conductivity, low concentrations of electron-withdrawing groups, and extensive surface area.
19 Increased basicity can enhance the dispersion of the active metal, thereby facilitating the
20 dehydrogenation of ammonia and the recombinative desorption of surface nitrogen atoms,
21 which are likely the rate-limiting steps of the reaction. Additionally, the electron-donating
22 characteristics of the catalyst can indirectly interact with the support to promote stronger
23 basicity. Consequently, adjusting the basicity of the supports is essential for developing
24 efficient catalysts for NH₃ decomposition. Beyond Ru and Ni catalysts, nitrides, carbides, and
25 perovskites have also gained popularity for optimizing active components in catalytic



1 processes. Looking ahead, it will be valuable to explore methods for separating and purifying
2 hydrogen derived from ammonia decomposition in a cost-effective and highly efficient
3 manner. Additionally, microwave and plasma-based decomposition of ammonia merits further
4 investigation.

5 Moreover, the economic evaluation of a large-scale NH_3 decomposition plant has revealed a
6 significant reliance on the cost of the green ammonia industry. It was demonstrated that lower
7 costs of renewable energy and green ammonia production lead to reduced hydrogen production
8 costs via ammonia decomposition. With a baseline price of green ammonia set at 450 €/ton,
9 the estimated levelized cost of hydrogen (LCOH) was approximately 4.82 € kg^{-1} (in 2019).
10 However, this estimate is influenced by several uncertainties, including the accuracy of total
11 investment cost estimation ($\pm 30\%$), the ammonia decomposition kinetics that affects cracker
12 size and consumption, and the use of ammonia/hydrogen blends as fuel for endothermic
13 reactions in conventional burners. In summary, if green ammonia becomes cost-competitive
14 with fossil-based ammonia, with an estimated price range of 210–215 € ton^{-1} , the cost of
15 producing pressurized hydrogen through ammonia decomposition would be approximately
16 3.00 €/kg, excluding any potential regulatory or financial incentives¹²⁰.

17

18 **8. Conclusions and Perspectives**

19 Ammonia, as an ideal hydrogen storage material, is expected to address the challenges of
20 hydrogen storage and transportation in the development of the hydrogen energy industry and
21 overcome the safety problems of hydrogen utilization. Although many ammonia-related
22 studies have contributed to the promotion of ammonia as a favorable alternative renewable
23 resource, further improvements are required in ammonia decomposition to make it a practical
24 H_2 carrier option for on-site generation.



1 Currently, the great potential of direct ammonia fuel cells for electricity generation in vehicles,
2 hydrogen refilling stations, and ammonia combustion for power requires the decomposition of
3 ammonia under mild conditions. Although progress toward the commercialization of direct
4 ammonia fuel cells is ongoing, in the future, within both distributed and grid power supply
5 systems, a carbon-neutral energy system that combines green ammonia synthesis with
6 ammonia fuel cell technology could become a reality.

7 In conclusion, combining ML with computational modeling or experiments opens up new
8 possibilities for rapid screening of the catalysts, identifying the performance descriptors, and
9 assisting in catalyst manufacturing. However, further steps are required to couple experimental
10 and theoretical techniques to gain a fundamental understanding, which will inspire researchers
11 to design advanced catalysts for mild-condition ammonia synthesis and decomposition.

13 **Data availability**

14 No primary research results, software or code, have been included and no new data was
15 generated or analyzed as part of this review.

17 **Conflicts of interest**

18 There are no conflicts to declare.

20 **Acknowledgements**

21 The authors acknowledge funding from the US National Science Foundation (NSF) grant (IIP
22 1939876). The NSF supported this study (Award numbers: 2315268—the Great Lakes Water
23 Innovation Engine and 2314720).



1 **References**

- 2 1. M. El-Shafie, S. Kambara, S. P. Katikaneni, S. N. Paglieri and K. Lee, *International Journal*
3 *of Hydrogen Energy*, 2024, **65**, 126-141.
- 4 2. X. Niu, C. Li, X. Li and Y. Zhang, *Heliyon*, 2024, **10**.
- 5 3. Z. Bao, D. Li, Z. Wang, Y. Wen, L. Jin and H. Hu, *Fuel*, 2024, **373**, 132346.
- 6 4. F. Schüth, R. Palkovits, R. Schlögl and D. S. Su, *Energy & Environmental Science*, 2012, **5**,
7 6278-6289.
- 8 5. J. Li, S. Lai, D. Chen, R. Wu, N. Kobayashi, L. Deng and H. Huang, *Frontiers in Energy*
9 *Research*, 2021, **9**, 760356.
- 10 6. C. Qin, S. Ruan, C. He and L. Zhang, *Colloids and Surfaces A: Physicochemical and*
11 *Engineering Aspects*, 2024, **691**, 133898.
- 12 7. N. Li, C. Zhang, D. Li, W. Jiang and F. Zhou, *Chemical Engineering Journal*, 2024, **495**,
13 153125.
- 14 8. M. Ghasemi, J. Choi, S. M. Ghoreishian, Y. S. Huh and H. Ju, *Journal of The*
15 *Electrochemical Society*, 2023, **170**, 074501.
- 16 9. N. Zhu, Y. Hong, F. Qian and J. Liang, *International Journal of Hydrogen Energy*, 2024, **59**,
17 791-807.
- 18 10. Z. Bao, D. Li, Y. Wu, L. Jin and H. Hu, *International Journal of Hydrogen Energy*, 2024, **53**,
19 848-858.
- 20 11. S. S. Rathore, S. Biswas, D. Fini, A. P. Kulkarni and S. Giddey, *International Journal of*
21 *Hydrogen Energy*, 2021, **46**, 35365-35384.
- 22 12. G. Glenk and S. Reichelstein, *Nature Energy*, 2019, **4**, 216-222.



- 1 13. Y. Gu, Y. Ma, Z. Long, S. Zhao, Y. Wang and W. Zhang, *International Journal of Hydrogen*
2 *Energy*, 2021, **46**, 4045-4054. View Article Online
DOI: 10.1039/D4CC06382A
- 3 14. K. Grubel, H. Jeong, C. W. Yoon and T. Autrey, *Journal of Energy Chemistry*, 2020, **41**, 216-
4 224.
- 5 15. I. Cabria, *International Journal of Hydrogen Energy*, 2024, **50**, 160-177.
- 6 16. Z. Yan, H. Liu, Z. Hao, M. Yu, X. Chen and J. Chen, *Chemical Science*, 2020, **11**, 10614-
7 10625.
- 8 17. C. Chen, K. Wu, H. Ren, C. Zhou, Y. Luo, L. Lin, C. Au and L. Jiang, *Energy & Fuels*, 2021,
9 **35**, 11693-11706.
- 10 18. P. Adamou, S. Bellomi, S. Hafeez, E. Harkou, S. M. Al-Salem, A. Villa, N. Dimitratos, G.
11 Manos and A. Constantinou, *Catalysis Today*, 2023, **423**, 114022.
- 12 19. A. Utsunomiya, A. Okemoto, Y. Nishino, K. Kitagawa, H. Kobayashi, K. Taniya, Y.
13 Ichihashi and S. Nishiyama, *Applied Catalysis B: Environmental*, 2017, **206**, 378-383.
- 14 20. S. Mukherjee, S. V. Devaguptapu, A. Sviripa, C. R. F. Lund and G. Wu, *Applied Catalysis B:*
15 *Environmental*, 2018, **226**, 162-181.
- 16 21. S. Sun, Q. Jiang, D. Zhao, T. Cao, H. Sha, C. Zhang, H. Song and Z. Da, *Renewable and*
17 *Sustainable Energy Reviews*, 2022, **169**, 112918.
- 18 22. S. F. Yin, B. Q. Xu, X. P. Zhou and C. T. Au, *Applied Catalysis A: General*, 2004, **277**, 1-9.
- 19 23. S. M. Ghoreishian, K. Shariati, Y. S. Huh and J. Lauterbach, *Chemical Engineering Journal*,
20 2023, **467**, 143533.
- 21 24. T. E. Bell and L. Torrente-Murciano, *Topics in Catalysis*, 2016, **59**, 1438-1457.



- 1 25. Y. Sun, W. Zeng, Y. Yang, Q. Wu and C. Zou, *Chemical Engineering Journal*, 2024, **502**, 158043. View Article Online
DOI: 10.1039/D4CC06382A
- 2
- 3 26. N. Morlanés, S. P. Katikaneni, S. N. Paglieri, A. Harale, B. Solami, S. M. Sarathy and J.
4 Gascon, *Chemical Engineering Journal*, 2021, **408**, 127310.
- 5 27. N. Zecher-Freeman, H. Zong, P. Xie and C. Wang, *Current Opinion in Green and
6 Sustainable Chemistry*, 2023, **44**, 100860.
- 7 28. Z.-W. Wu, X. Li, Y.-H. Qin, L. Deng, C.-W. Wang and X. Jiang, *International Journal of
8 Hydrogen Energy*, 2020, **45**, 15263-15269.
- 9 29. K. G. Kirste, K. McAulay, T. E. Bell, D. Stoian, S. Laassiri, A. Daisley, J. S. J. Hargreaves,
10 K. Mathisen and L. Torrente-Murciano, *Applied Catalysis B: Environmental*, 2021, **280**,
11 119405.
- 12 30. N. Morlanés, S. Sayas, G. Shterk, S. P. Katikaneni, A. Harale, B. Solami and J. Gascon,
13 *Catalysis Science Technology*, 2021, **11**, 3014-3024.
- 14 31. E. Fu, Y. Qiu, H. Lu, S. Wang, L. Liu, H. Feng, Y. Yang, Z. Wu, Y. Xie, F. Gong and R.
15 Xiao, *Fuel Processing Technology*, 2021, **221**, 106945.
- 16 32. I. Lucentini, A. Casanovas and J. Llorca, *International Journal of Hydrogen Energy*, 2019,
17 **44**, 12693-12707.
- 18 33. V. D. B. C. Dasireddy, Š. Hajduk, F. Ruiz-Zepeda, J. Kovač, B. Likozar and Z. C. Orel, *Fuel
19 Processing Technology*, 2021, **215**, 106752.
- 20 34. T. Han, L. Wei, S. Xie, Y. Liu, H. Dai and J. Deng, *Industrial Chemistry & Materials*, 2025.
- 21 35. Z. Zhao, Z. Liu, M. Li, Y. Yang, L. Deng, Y. Zhao, B. Dou and F. Bin, *Separation and
22 Purification Technology*, 2025, **360**, 131144.



- 1 36. D. Liang, C. Feng, L. Xu, D. Wang, Y. Liu, X. Li and Z. Wang, *Catalysis Science & Technology*, 2023, **13**, 3614-3628. View Article Online
DOI: 10.1039/D4CC06382A
- 2
- 3 37. J. C. Verschoor, P. E. de Jongh and P. Ngene, *Current Opinion in Green and Sustainable Chemistry*, 2024, **50**, 100965.
- 4
- 5 38. Y. Qiu, E. Fu, F. Gong and R. Xiao, *International Journal of Hydrogen Energy*, 2022, **47**,
- 6 5044-5052.
- 7 39. G. Li, H. Zhang, X. Yu, Z. Lei, F. Yin and X. He, *International Journal of Hydrogen Energy*,
- 8 2022, **47**, 12882-12892.
- 9 40. H. Tang, Y. Wang, W. Zhang, Z. Liu, L. Li, W. Han and Y. Li, *Journal of Solid State Chemistry*, 2021, **295**, 121946.
- 10
- 11 41. G. Li, X. Yu, F. Yin, Z. Lei, H. Zhang and X. He, *Catalysis Today*, 2022, **402**, 45-51.
- 12 42. M. Pinzón, O. Avilés-García, A. R. de la Osa, A. de Lucas-Consuegra, P. Sánchez and A. Romero, *Sustainable Chemistry and Pharmacy*, 2022, **25**, 100615.
- 13
- 14 43. A. Jedynek, Z. Kowalczyk, D. Szmigiel, W. Raróg and J. Zieliński, *Applied Catalysis A: General*, 2002, **237**, 223-226.
- 15
- 16 44. J. C. Ganley, F. Thomas, E. Seebauer and R. I. J. C. L. Masel, 2004, **96**, 117-122.
- 17 45. H. Li, L. Guo, J. Qu, X. Fang, Y. Fu, J. Duan, W. Wang and C. Li, *International Journal of Hydrogen Energy*, 2023, **48**, 8985-8996.
- 18
- 19 46. J. Zhang, M. Comotti, F. Schüth, R. Schlögl and D. S. Su, *Chemical Communications*, 2007,
- 20 1916-1918.
- 21 47. L. Li, F. Chen, J. Shao, Y. Dai, J. Ding and Z. Tang, *International Journal of Hydrogen Energy*, 2016, **41**, 21157-21165.
- 22



- 1 48. M. Feyen, C. Weidenthaler, R. Güttel, K. Schlichte, U. Holle, A.-H. Lu and F. Schüth, *Chemistry – A European Journal*, 2011, **17**, 598-605. View Article Online
DOI: 10.1039/D4CC06382A
- 2
- 3 49. H. Zhang, Y. A. Alhamed, A. Al-Zahrani, M. Daous, H. Inokawa, Y. Kojima and L. A. Petrov, *International Journal of Hydrogen Energy*, 2014, **39**, 17573-17582.
- 4
- 5 50. T. A. Le, Y. Kim, H. W. Kim, S.-U. Lee, J.-R. Kim, T.-W. Kim, Y.-J. Lee and H.-J. Chae, *Applied Catalysis B: Environmental*, 2021, **285**, 119831.
- 6
- 7 51. S. Podila, Y. A. Alhamed, A. A. AlZahrani and L. A. Petrov, *International Journal of Hydrogen Energy*, 2015, **40**, 15411-15422.
- 8
- 9 52. M. Pinzón, A. Romero, A. de Lucas-Consuegra, A. R. de la Osa and P. Sánchez, *Catalysis Today*, 2022, **390-391**, 34-47.
- 10
- 11 53. K. Okura, T. Okanishi, H. Muroyama, T. Matsui and K. Eguchi, *Applied Catalysis A: General*, 2015, **505**, 77-85.
- 12
- 13 54. N. Zhu, F. Yang, Y. Hong and J. Liang, *International Journal of Hydrogen Energy*, 2025, **98**, 1243-1261.
- 14
- 15 55. I. Lucentini, X. Garcia, X. Vendrell, J. J. I. Llorca and E. C. Research, 2021, **60**, 18560-18611.
- 16
- 17 56. X. Huang, K. Lei, Y. Mi, W. Fang and X. Li, *Molecules*, 2023, **28**, 5245.
- 18 57. S. Mirsadeghi, S. M. Ghoreishian, H. Zandavar, R. Behjatmanesh-Ardakani, E. Naghian, M. Ghoreishian, A. Mehrani, N. Abdolhoseinpoor, M. R. Ganjali, Y. S. Huh and S. M. Pourmortazavi, *Journal of Environmental Chemical Engineering*, 2023, **11**, 109106.
- 19
- 20
- 21 58. S. M. Ghoreishian, K. S. Ranjith, B. Park, S.-K. Hwang, R. Hosseini, R. Behjatmanesh-Ardakani, S. M. Pourmortazavi, H. U. Lee, B. Son, S. Mirsadeghi, Y.-K. Han and Y. S. Huh, *Chemical Engineering Journal*, 2021, **419**, 129530.
- 22
- 23



- 1 59. S. M. Ghoreishian, K. S. Ranjith, M. Ghasemi, B. Park, S.-K. Hwang, N. Irannejad, M. Norouzi, S. Y. Park, R. Behjatmanesh-Ardakani, S. M. Pourmortazavi, S. Mirsadeghi, Y.-K. Han and Y. S. Huh, *Chemical Engineering Journal*, 2023, **452**, 139435. View Article Online
DOI: 10.1039/D4CC06382A
- 2
- 3
- 4 60. H. Martin, C. Ruck, M. Schmidt, S. Sell, S. Beutner, B. Mayer and R. Walsh, *Pure and Applied Chemistry*, 1999, **71**, 2253-2262.
- 5
- 6 61. B. G. Petri, R. J. Watts, A. L. Teel, S. G. Huling and R. A. Brown, in *In situ chemical oxidation for groundwater remediation*, 2011, pp. 33-88.
- 7
- 8 62. Z. Yong and T. Ma, *Angewandte Chemie International Edition*, 2023, **62**, 202308980.
- 9 63. M. Reli, M. Edelmannová, M. Šihor, P. Praus, L. Svoboda, K. K. Mamulová, H. Otoupalíková, L. Čapek, A. Hospodková, L. Obalová and K. Kočí, *International Journal of Hydrogen Energy*, 2015, **40**, 8530-8538.
- 10
- 11
- 12 64. H. Kominami, H. Nishimune, Y. Ohta, Y. Arakawa and T. Inaba, *Applied Catalysis B: Environmental*, 2012, **111-112**, 297-302.
- 13
- 14 65. C. Jo, S. Surendran, M.-C. Kim, T.-Y. An, Y. Lim, H. Choi, G. Janani, S. Cyril Jesudass, D. Jun Moon, J. Kim, J. Young Kim, C. Hyuck Choi, M. Kim, J. Kyu Kim and U. Sim, *Chemical Engineering Journal*, 2023, **463**, 142314.
- 15
- 16
- 17 66. H. Shi, C. Li, L. Wang, W. Wang, J. Bian and X. Meng, *Journal of Alloys and Compounds*, 2023, **933**, 167815.
- 18
- 19 67. D. Yuan, F. Xie, K. Li, Q. Guan, J. Hou, S. Yang, G. Han, X. San, J. Hao and Y. Li, *Applied Surface Science*, 2023, **613**, 155973.
- 20
- 21 68. S. Zhang, Z. He, X. Li, J. Zhang, Q. Zang and S. Wang, *Nanoscale Advances*, 2020, **2**, 3610-3623.
- 22



- 1 69. J. Lin, Y. Wang, W. Tian, H. Zhang, H. Sun and S. Wang, *ACS Catalysis*, 2023, **13**, 11711-11722. New Article Online
DOI: 10.1039/D4CC06382A
- 2 11722.
- 3 70. J. Dzibelová, S. M. H. Hejazi, V. Šedajová, D. Panáček, P. Jakubec, Z. Baďura, O. Malina, J.
4 Kašlík, J. Filip, Š. Kment, M. Otyepka and R. Zbořil, *Applied Materials Today*, 2023, **34**,
5 101881.
- 6 71. S. Zhang, L. Yan, H. Jiang, L. Yang, Y. Zhao, X. Yang, Y. Wang, J. Shen and X. Zhao, *ACS*
7 *Applied Materials & Interfaces*, 2022, **14**, 9036-9045.
- 8 72. Z. Wang, S. D. Young, B. R. Goldsmith and N. Singh, *Journal of Catalysis*, 2021, **395**, 143-
9 154.
- 10 73. Y. Tian, Z. Mao, L. Wang and J. Liang, *Small Structures*, 2023, **4**, 2200266.
- 11 74. R. Sen, S. Das, A. Nath, P. Maharana, P. Kar, F. Verpoort, P. Liang and S. Roy, *Frontiers in*
12 *Chemistry*, 2022, **10**, 861604.
- 13 75. A. AlZaabi, F. AlMarzooqi and D. Choi, *International Journal of Hydrogen Energy*, 2024,
14 **94**, 23-52.
- 15 76. K. Goshome, T. Yamada, H. Miyaoka, T. Ichikawa and Y. Kojima, *International Journal of*
16 *Hydrogen Energy*, 2016, **41**, 14529-14534.
- 17 77. N. Hanada, S. Hino, T. Ichikawa, H. Suzuki, K. Takai and Y. Kojima, *Chemical*
18 *communications*, 2010, **46**, 7775-7777.
- 19 78. Z. Wu, N. Ambrožová, E. Eftekhari, N. Aravindakshan, W. Wang, Q. Wang, S. Zhang, K.
20 Kočí and Q. Li, *Emergent Materials*, 2019, **2**, 303-311.
- 21 79. N. M. Adli, H. Zhang, S. Mukherjee and G. Wu, *Journal of The Electrochemical Society*,
22 2018, **165**, J3130.



- 1 80. J.-J. Zhong, S.-P. Huang, J.-F. Gu, Y. Li, K.-N. Ding, Y.-F. Zhang, W. Lin and W.-K. Chen, *Applied Surface Science*, 2023, **609**, 155280. View Article Online
DOI: 10.1039/D4CC06382A
- 2
- 3 81. J. A. Herron, P. Ferrin and M. Mavrikakis, *The Journal of Physical Chemistry C*, 2015, **119**,
- 4 14692-14701.
- 5 82. P. Modisha and D. Bessarabov, *International Journal of Electrochemical Science*, 2016, **11**,
- 6 6627-6635.
- 7 83. B.-X. Dong, H. Tian, Y.-C. Wu, F.-Y. Bu, W.-L. Liu, Y.-L. Teng and G.-W. Diao,
- 8 *International Journal of Hydrogen Energy*, 2016, **41**, 14507-14518.
- 9 84. M. Idamakanti, E. B. Ledesma, R. R. Ratnakar, M. P. Harold, V. Balakotaiah and P. Bollini,
- 10 *ACS Engineering Au*, 2023, **4**, 71-90.
- 11 85. Y.-S. Son, K.-H. Kim, K.-J. Kim and J.-C. Kim, *Plasma Chemistry and Plasma Processing*,
- 12 2013, **33**, 617-629.
- 13 86. D. Varisli, C. Korkusuz and T. Dogu, *Applied Catalysis B: Environmental*, 2017, **201**, 370-
- 14 380.
- 15 87. M. Akiyama, K. Aihara, T. Sawaguchi, M. Matsukata and M. Iwamoto, *International Journal*
- 16 *of Hydrogen Energy*, 2018, **43**, 14493-14497.
- 17 88. P. Peng, J. Su and H. Breunig, *Energy Conversion and Management*, 2023, **288**, 117166.
- 18 89. Z. Wang, H. Zhang, Z. Ye, G. He, C. Liao, J. Deng, G. Lei, G. Zheng, K. Zhang, F. Gou and
- 19 X. Mao, *International Journal of Hydrogen Energy*, 2024, **49**, 1375-1385.
- 20 90. K. H. R. Rouwenhorst, Y. Engelmann, K. van 't Veer, R. S. Postma, A. Bogaerts and L.
- 21 Lefferts, *Green Chemistry*, 2020, **22**, 6258-6287.



- 1 91. L. Wang, Y. Yi, Y. Zhao, R. Zhang, J. Zhang and H. Guo, *ACS Catalysis*, 2015, **5**, 4167-4174. View Article Online
DOI: 10.1039/D4CC06382A
- 2 4174.
- 3 92. N. Wang, H. O. Otor, G. Rivera-Castro and J. C. Hicks, *ACS Catalysis*, 2024, **14**, 6749-6798.
- 4 93. J. Moszczyńska, X. Liu and M. Wiśniewski, *International Journal of Molecular Sciences*,
- 5 2022, **23**, 9638.
- 6 94. S. Shibuya, Y. Sekine and I. Mikami, *Applied Catalysis A: General*, 2015, **496**, 73-78.
- 7 95. M. Reli, N. Ambrožová, M. Šihor, L. Matějová, L. Čapek, L. Obalová, Z. Matěj, A. Kotarba
- 8 and K. Kočí, *Applied Catalysis B: Environmental*, 2015, **178**, 108-116.
- 9 96. Y.-N. Li, Z.-Y. Chen, S.-J. Bao, M.-Q. Wang, C.-L. Song, S. Pu and D. Long, *Chemical*
- 10 *Engineering Journal*, 2018, **331**, 383-388.
- 11 97. S. Pu, D. Long, M.-Q. Wang, S.-J. Bao, Z. Liu, F. Yang, H. Wang and Y. Zeng, *Materials*
- 12 *Letters*, 2017, **209**, 56-59.
- 13 98. H. Zhang, Q.-Q. Gu, Y.-W. Zhou, S.-Q. Liu, W.-X. Liu, L. Luo and Z.-D. Meng, *Applied*
- 14 *Surface Science*, 2020, **504**, 144065.
- 15 99. R. Wang, T. Xie, Z. Sun, T. Pu, W. Li and J.-P. Ao, *RSC advances*, 2017, **7**, 51687-51694.
- 16 100. W. Guo and H. Liu, *Chemical Research in Chinese Universities*, 2017, **33**, 129-134.
- 17 101. B. Achrai, Y. Zhao, T. Wang, G. Tamir, R. Abbasi, B. P. Setzler, M. Page, Y. Yan and S.
- 18 Gottesfeld, *Journal of The Electrochemical Society*, 2020, **167**, 134518.
- 19 102. L. Cunci, C. V. Rao, C. Velez, Y. Ishikawa and C. R. Cabrera, *Electrocatalysis*, 2013, **4**, 61-
- 20 69.
- 21 103. J. C. M. Silva, S. Ntais, É. Teixeira-Neto, E. V. Spinacé, X. Cui, A. O. Neto and E. A.
- 22 Baranova, *International Journal of Hydrogen Energy*, 2017, **42**, 193-201.



- 1 104. N. Sacré, M. Duca, S. Garbarino, R. Imbeault, A. Wang, A. Hadj Youssef, J. Galipaud, C. View Article Online
2 Hufnagel, A. Ruediger and L. Roue, *ACS Catalysis*, 2018, **8**, 2508-2518. DOI: 10.1039/D4CC06382A
- 3 105. L. Wang, Y. Zhao, C. Liu, W. Gong and H. Guo, *Chemical communications*, 2013, **49**, 3787-
4 3789.
- 5 106. Q. F. Lin, Y. M. Jiang, C. Z. Liu, L. W. Chen, W. J. Zhang, J. Ding and J. G. Li, *Energy*
6 *Reports*, 2021, **7**, 4064-4070.
- 7 107. M. El-Shafie, S. Kambara and Y. Hayakawa, *Journal of the Energy Institute*, 2021, **99**, 145-
8 153.
- 9 108. J. A. Andersen, K. van 't Veer, J. M. Christensen, M. Østberg, A. Bogaerts and A. D. Jensen,
10 *Chemical Engineering Science*, 2023, **271**, 118550.
- 11 109. Y. Hayakawa, S. Kambara and T. Miura, *International Journal of Hydrogen Energy*, 2020,
12 **45**, 32082-32088.
- 13 110. B. Yan, Y. Li, W. Cao, Z. Zeng, P. Liu, Z. Ke and G. Yang, *Journal of the American*
14 *Chemical Society*, 2024, **146**, 4864-4871.
- 15 111. J. C. McLennan and G. Greenwood, *Proceedings of the Royal Society of London*, 1928, **120**,
16 283-295.
- 17 112. S. Hirabayashi and M. Ichihashi, *International Journal of Mass Spectrometry*, 2016, **407**, 86-
18 91.
- 19 113. W. Guo, A. Shafizadeh, H. Shahbeik, S. Rafiee, S. Motamedi, S. A. Ghafarian Nia, M. H.
20 Nadian, F. Li, J. Pan, M. Tabatabaei and M. Aghbashlo, *Journal of Energy Storage*, 2024, **89**,
21 111688.
- 22 114. E. Soltanmohammadi and N. Hikmet, *Journal of Data Analysis Information Processing*,
23 2024, **12**, 544-565.



- 1 115. E. Soltanmohammadi, A. Dilek and N. Hikmet, *Journal of Data Analysis Information Processing*, 2024, **13**, 46-65. View Article Online
DOI: 10.1039/D4CC06382A
- 2
- 3 116. D.-N. Vo, J. Hun Chang, S.-H. Hong and C.-H. Lee, *Chemical Engineering Journal*, 2023,
4 **475**, 146195.
- 5 117. T. Williams, K. McCullough and J. A. Lauterbach, *Chemistry of Materials*, 2019, **32**, 157-
6 165.
- 7 118. Z.-H. Lyu, J. Fu, T. Tang, J. Zhang and J.-S. Hu, *EnergyChem*, 2023, **5**, 100093.
- 8 119. H. Mashhadimoslem, M. Safarzadeh Khosrowshahi, M. Delpisheh, C. Convery, M.
9 Rezakazemi, T. M. Aminabhavi, M. Kamkar and A. Elkamel, *Chemical Engineering Journal*,
10 2023, **474**, 145661.
- 11 120. C. Makhoulfi and N. Kezibri, *International Journal of Hydrogen Energy*, 2021, **46**, 34777-
12 34787.
- 13



No primary research results, software or code have been included and no new data were generated or analysed as part of this review.

